Investigating the Pathogenicity of *VSX1* Missense Mutations and Their Association With Corneal Disease

Anastasia Marie Litke,[1] Sarah Samuelson,[2] Kerry R. Delaney,[1] Yves Sauvé,[2] and Robert L. Chow[1]

[1]Department of Biology, University of Victoria, Victoria, British Columbia, Canada
[2]Department of Ophthalmology and Visual Sciences, University of Alberta, Edmonton, Alberta, Canada

Correspondence: Robert L. Chow, Department of Biology, University of Victoria, Cunningham 202, Victoria, BC V8W 2Y2, Canada; bobchow@uvic.ca.

Submitted: August 13, 2018
Accepted: October 29, 2018

Citation: Litke AM, Samuelson S, Delaney KR, Sauvé Y, Chow RL. Investigating the pathogenicity of *VSX1* missense mutations and their association with corneal disease. *Invest Ophthalmol Vis Sci*. 2018;59:5824–5835. https://doi.org/10.1167/iovs.18-25490

Purpose. Despite numerous studies associating Visual System Homeobox 1 (*VSX1*), with posterior polymorphous corneal dystrophy and keratoconus, its role in these diseases is unclear. Here we examine the pathogenicity of *VSX1* missense mutations in vitro and in a mouse genetic model.

Methods. Vsx1 transcriptional repressor activity, protein stability, and subcellular localization activity, was examined using luciferase reporter-based assays, western blotting and immunolabeling, respectively, in transfected human embryonic kidney 293T cells. A genetic model for *VSX1* p.P247R was generated to investigate pathogenicity of the mutation, in vivo. A wholemount confocal imaging approach on unfixed intact eyes was developed to examine corneal morphology, curvature, and thickness. Immunolabeling and electroretinography was used to examine retinal phenotype.

Results. A mutation corresponding to human *VSX1* p.P247R led to enhanced transcriptional repressor activity, in vitro. A mouse model for *VSX1* p.P247R did not have any observable corneal defect, but did exhibit an abnormal electroretinogram response characterized by a more prominent ON as opposed to OFF panretinal responsiveness. In vitro analysis of additional *VSX1* missense mutations showed that they either enhanced repressor activity or did not alter activity.

Conclusions. Our results indicate that although *VSX1* sequence variants can alter transcriptional activity, in the context of a mouse genetic model, at least one of these changes does not lead to corneal abnormalities. While we cannot exclude a role for *VSX1* as a risk factor for corneal disease, on its own, it does not appear to play a major causative role.

Keywords: Vsx1, cornea, posterior polymorphism dystrophy, keratoconus, retina, mouse model

Corneal dystrophies are classified as a group of inherited diseases that result in damage to the visual system through slowly progressive, bilateral, symmetric and non-inflammatory changes to cornea structure.[1] One of these, posterior polymorphous corneal dystrophy (PPCD), is characterized by opacities in the cornea due to changes of the Descemet membrane and endothelium due to the mesenchymal-like transformation and proliferation of the innermost endothelial monolayer.[1–3] In many cases, PPCD has been associated with the corneal disease keratoconus.[4–10] Keratoconus results from a bilateral, noninflammatory thinning of the central stromal layer of the cornea which results in severe astigmatism.[11] While not currently classified as a corneal dystrophy due to uncertainty surrounding its inheritance pattern and lack of convincing molecular genetic evidence supporting either dominant or recessive modes of inheritance, 10% of keratoconus cases do have a positive family history.[1,12–15]

Linkage of PPCD1 (MIM: 122000) to 20p11-q11,[16] initially led to the screening of the paired-like homeodomain transcription factor-encoding ocular gene, Visual Systems Homeobox 1 (*VSX1*).[16] Although this initial linkage group did not reveal *VSX1* mutations, a subsequent study identified six mutations spanning the protein coding sequence of *VSX1* associated with PPCD and/or keratoconus.[16] Since this study, 18 studies have identified a total of 20 *VSX1* missense mutations associated with corneal disease (Table 1).[17–33] Eight of these mutations are of highly conserved amino acids within the homeodomain and CVC domain (Fig. 1).

Despite the identification of many *VSX1* missense changes in disease populations, there is uncertainty with regard to their pathogenicity. For instance, several of the *VSX1* changes that were identified above have also been identified in unaffected individuals or control groups[18,20,24,26,29–31,33–36] (see Table 1) and other studies mapping PPCD1 to chromosome 20 have excluded *VSX1* and identified *OVOL2* as the causative gene.[34,37,38] In addition, *VSX1*/*Vsx1* mRNA, protein or reporter gene expression has not been detected in either the human or mouse cornea,[31,39] and no overt corneal phenotypes have been reported in *Vsx1*-null mice.[40]

In contrast to its unclear role in corneal disease, *Vsx1* function has been well characterized in the mouse retina. *Vsx1* is expressed in a subset of postmitotic cone bipolar cells and is essential for their terminal differentiation.[40–43] Mice lacking *Vsx1* exhibit ERG b-wave defects, decreased OFF visual signaling, and a perturbation of directional selectivity, all of which are thought to arise from dysfunctional cone bipolar cell signaling.[40,41,43] *VSX1* mutations in humans have also been associated with visual signaling defects and individuals with *VSX1* mutations have exhibited an abnormal ERG b-wave

Table 1. Summary of Studies That Have Identified *VSX1* Mutations in Keratoconus and PPCD Disease Populations

Variant*	Allele Frequency†	Disease Phenotype	Affected With Variant, *n*	Total Affected Screened, *n*	Familial History	Control Individuals Tested, *n* (Positive)	Author Conclusion	Source
p.L17P	1.12×10^{-4}	Keratoconus	3	80	Yes	125 (0)	Pathogenic	17
		Keratoconus	2	225/77‡	1/2 Patients	200 (0)	Possibly Pathogenic	18
p.L17V	7.75×10^{-4}	Keratoconus	2	53	11/53 Patients	100 (1)	Nonpathogenic	26
p.P58L	3.24×10^{-5}	PPCD	1	47	16/47 Patients	100 (0)	Pathogenic	27
p.D105E	6.89×10^{-3}	Keratoconus	2	85§	Yes	50 (0)	Nonpathogenic	36
p.R131S	1.00×10^{-5}	PPCD*	4	7	Yes	624 (5)	Nonpathogenic	29
		Keratoconus	1	100	Unknown	None Studied	Nonpathogenic	13
		Keratoconus	5	85§	Yes	50 (0)	Nonpathogenic	36
p.D144E	3.35×10^{-3}	Both	1	85	Yes	277 (0)	Possibly Pathogenic	61
		PPCD	1	19	Yes	102 (1)	Nonpathogenic	30
		Keratoconus	2	80	Yes	125 (0)	Pathogenic	17
		Keratoconus	1	100	No	None Studied	Nonpathogenic	13
		Keratoconus	7	10	Yes	104 (1)	Pathogenic	62
		Keratoconus	0	39/27‡	Yes	100 (0)‖	Nonpathogenic	33
		Keratoconus	3	225/77‡	No	200 (1)	Possibly Pathogenic	18
		Keratoconus	2	85§	Yes	50 (0)‖	Nonpathogenic	36
p.N151S	7.28×10^{-5}	Keratoconus	1	249	Unknown	249 (0)	Pathogenic	19
p.L159M	4.36×10^{-5}	Keratoconus	1	85	Yes	277 (0)	Pathogenic	61
		Keratoconus	3	444	No and Yes	71 (1)‖	Nonpathogenic	20
p.G160D	2.06×10^{-3}	PPCD*	1	85	Yes	277 (0)	Pathogenic	61
		Keratoconus	2	80	Yes	125 (0)	Pathogenic	17
		Keratoconus	1	225/77‡	No	200 (0)	Possibly Pathogenic	18
		Keratoconus	2	39/27‡	No	100 (0)	Possibly Pathogenic	33
p.G160V	9.70×10^{-4}	Keratoconus	13	249	Unknown	249 (0)	Pathogenic	19
		Keratoconus	3	53	11/53 Patients	100 (3)	Nonpathogenic	26
p.**R166W**	2.19×10^{-5}	Keratoconus	1	85	No	277 (0)	Pathogenic	61
		Keratoconus	1	112	Yes	100 (0)	Possibly Pathogenic	21
p.**Q175H**	4.06×10^{-6}	Keratoconus	1	66	No	100	Possibly Pathogenic	63
p.V199L	3.25×10^{-5}	Keratoconus	1	53	11/53 Patients	100 (0)‖	Nonpathogenic	26
p.R217H¶	0.21	Keratoconus	1	39/27‡	No	100 (22)	Nonpathogenic	33
		Keratoconus	1	50	No	50 (0)	Nonpathogenic	23
		Keratoconus	18	85§	Yes	50 (0)	Nonpathogenic	36
p.**G239R**	2.24×10^{-5}	Keratoconus	1	225/77‡	Yes	200 (0)	Possibly Pathogenic	18
p.**H244R**	2.63×10^{-3}	Keratoconus	1	85	Yes	277 (2)	Possibly Pathogenic	61
		PPCD‖	8	9	Yes	None Studied	Pathogenic	24
		Keratoconus	2	444	Yes	71 (0)‖	Nonpathogenic	20
		Keratoconus	1	112	Yes	100 (0)	Possibly Pathogenic	21
		Keratoconus	1	47	No	100 (0)	Pathogenic	27
p.**P247R**	4.49×10^{-4}	PPCD	1	85	No	196 (0)	Possibly Pathogenic	61
		Keratoconus	1	80	Yes	125 (0)	Pathogenic	17
		Keratoconus	4	225/77‡	Yes	200 (0)	Possibly Pathogenic	18
		None	0	85§	No	50 (1)	Nonpathogenic	36
p.S251T	Not documented	Keratoconus	3	20	Yes	105 (0)	Nonpathogenic	25
p.**A256S**	1.59×10^{-4}	PPCD‖	4	7	Yes	624 (0)	Pathogenic	29
p.L268H	Not documented	Keratoconus	5	20	Yes	105 (0)	Possibly Pathogenic	25

All mutations identified, in patients and controls, are found in a heterozygous form. Mutations in bold are of highly conserved amino acids located within the homeodomain or CVC domain examined in this study. R131S PPCD* and A245S PPCD* were identified in individuals with additional visual, auditory and craniofacial deficits. D144E Keratoconus* and P247R None* were identified in individuals with abnormal ERGs.

* Unless otherwise noted, variants are of *VSX1* splice variant 1 (NM_014588.5).

† Allele frequency was mined from gnomAD, r2.0.2 (http://gnomad.broadinstitute.org).

‡ Indicates number of patients studied in each category of keratoconus (sporadic/familial).

‖ Indicates studies where mutations were found in unaffected family members.

¶ Reference SNP ID rs6138482 is located in non-canonical *VSX1* splice variant 2 (a readthrough of exon 3).

§ Study looked at two or more affected individuals from 85 families.

consistent with a defect in retinal bipolar interneuron function.[24,29,31]

Here, we examine the pathogenicity of PPCD- and keratoconus-associated *VSX1* missense mutations. Our study was performed within the context of the mouse and utilized both in vitro cell-based luciferase reporter assays as well as the generation of a genetic animal model. The primary focus of this study was NM_014588.5:c.740C > G (p.P247R), herein referred to as *VSX1* p.P247R, as this mutation has been associated with PPCD, keratoconus and retinal function.[17,18,31] We also examined several other *VSX1* mutations that reside at highly conserved amino acid residues. Our results indicate that although disease-associated *VSX1* mutations alter transcriptional activity, in the context of the mouse, in vivo, at least

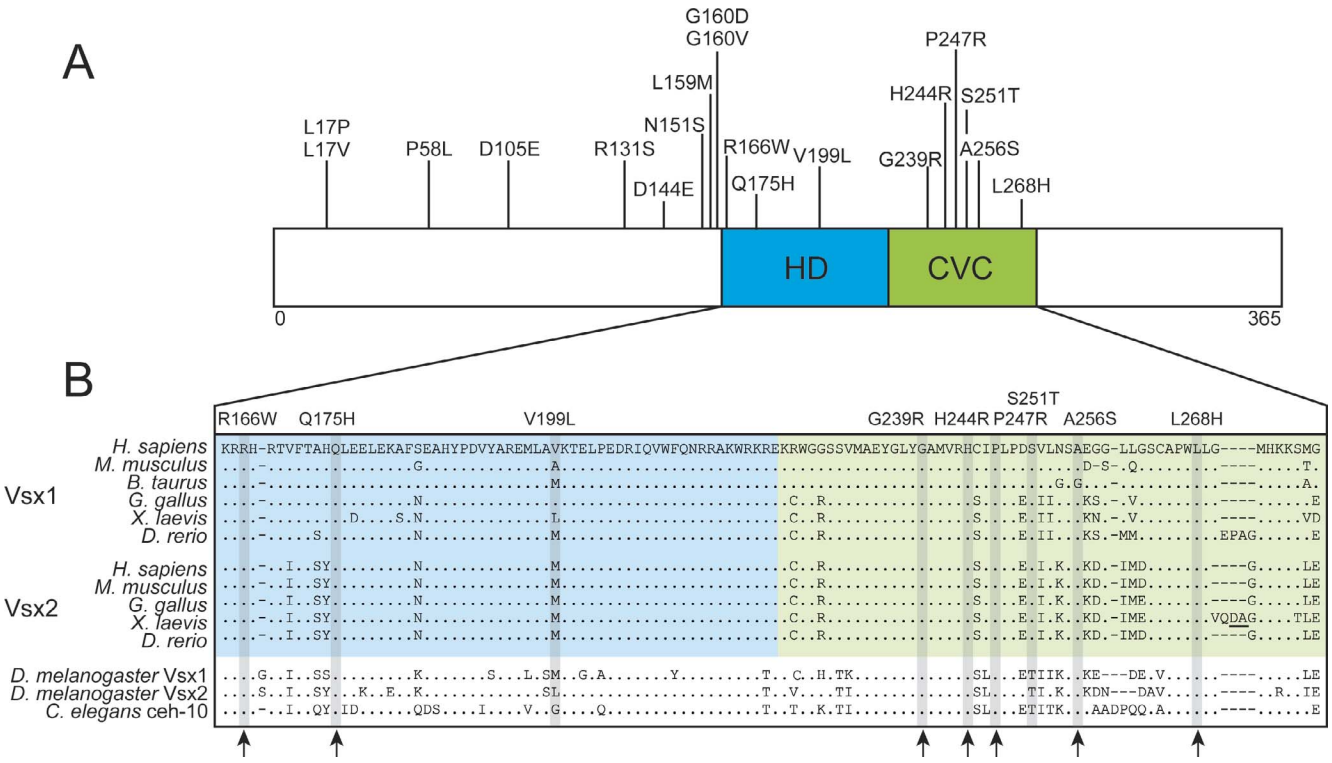

Figure 1. Summary of VSX1 mutations implicated in the corneal dystrophies PPCD and keratoconus. (**A**) Distribution of human VSX1 mutations implicated in PPCD and keratoconus (homeodomain, *blue*; CVC domain, *green*). (**B**) Amino acid alignment of the homeodomains (*blue*) and CVC domains (*green*) of VSX1, VSX2 and other invertebrate Prd-L:CVC homologues. *Red dots* under the alignment indicate mutation of residues that are conserved in vertebrate and invertebrate Prd-L:CVC homologues.

p.P247R does not lead to corneal disease. These findings are consistent with evidence from the literature that *VSX1*, on its own, does not play a major causal role in corneal disease.

Materials and Methods

Mice

All mice in this study were maintained on a 12-hour light/dark cycle. All experimental procedures were approved by the University of Victoria Animal Care Committee, in accordance with the Canadian Council for Animal Care (Protocol Number: 2014-023) and adhered to the ARVO Statement for the Use of Animals in Ophthalmic and Vision Research. *Vsx1*-null mice[40] and *GUS8.4GFP* mice[44] (provided by R. Margolskee) were maintained on a 129S1 background and genotyped as previously described.[40,44]

Generation of Vsx1 P254R Mice

Vsx1^{P254R} mice were generated using clustered regularly interspaced short palindromic repeats (CRISPR)-Cas9 gene editing on a C57BL/6 background at the University of Cincinnati Children's Hospital Transgenic Core Facility. A CCA to AGG mutation at Vsx1 amino acid position 254 (corresponding to human *VSX1* p.P247), was mediated by the gRNA 5′-CTGCATTCCACTGCCGGA-3′. The donor template included, in addition to the intended missense mutation, an additional silent mutation of CTG to CTT (leucine) at amino acid position 255 to create a BspE1 restriction enzyme site which allows the *P254R* allele to be distinguished from wild type. Four potential founder lines were generated are crossed to wild-type C57Bl/6 mice. Offspring were genotyped and sequenced to confirm the presence of the mutations and rule out any off-target mutations that may have been introduced. Two independent lines harboring both the p.P254R mutation and the silent CTG to CTT genotyping mutation were established. *Vsx1*^{P254R} mice were genotyped by amplifying genomic DNA with the following primers: forward primer: GAGTGGTCCCTTTGTAGACCC, reverse primer: ATA CATTGCCTCACAGTTTCAACA, and digesting PCR products with BspE1 prior to gel electrophoresis.

Plasmids

5xGal4-4xP3-TATA-luciferase was built from an original reporter plasmid 5xGAL4-TATA-luciferase (Addgene # 46756). Four *Vsx1*-interacting P3 binding sites separated by 8 base pairs (bp), of sequence 5′-TAATTAAATTA-3′, were introduced downstream from five Gal4-binding sites and upstream from the TATA promoter. Original P3 sequence and 8-bp separator sequence were obtained from HD4pG5EC (built by J. Epstein). All plasmid modifications were confirmed by sequencing. pBXG6-HSF1 is a Gal4-HSF1 activator fusion construct containing Gal4(1-147) and residues 201-529 of the heat shock factor 1 (HSF1, provided by R. Bremner; Mt. Sinai Hospital, Toronto, Canada). *Vsx1* expression constructs were generated by Haiquan Liu (Chow Lab). p.R173W, p.Q182H, p.G246R, p.H251R, p.P254R and p.A263S were introduced into wild-type *Vsx1* (Table 2) by site-directed mutagenesis using commercial software (NEBaseChanger; New England Biolabs, Inc., Ipswich, MA, USA) to design mutagenesis primers and a commercial kit (Q5 Site-Directed Mutagenesis kit; New England Biolabs, Inc.) to introduce mutations. To allow for Western blotting and cell immunocytochemistry, an HSV tag was cloned into pEF-*Vsx1* construct by site-directed mutagenesis in the same way as the untagged expression constructs.

Table 2. Mouse Mutations Corresponding to Highly Conserved Human *VSX1* Mutations Associated With PPCD and Keratoconus

Human Variant (NM_014588.5)	Mouse Variant	Sequence	
		Wild-Type	Mutant
p.R166W	p.R173W	AGG	UGG
p.Q175H	p.Q182H	CAA	CAC
p.G239R	p.G246R	GGA	AGA
p.H244R	p.H251R	CAC	AGG
p.P247R	p.P254R	CCA	AGG
p.A256S	p.A263S	GCA	AGC

Cell Lines

Human embryonic kidney (HEK) 293T cells were grown on 10 cm plates in Dulbecco's Modified Eagle Medium supplemented with 10% fetal bovine serum, 1% L-glutamine and 1% penicillin-streptomycin at 37°C, 5% CO2.

UAS Luciferase Reporter Assay

HEK 293T cells were trypsinized and plated on 96 well plates at a seeding density of 0.025×10^6 cells/well. Plates were left for 24 hours before transfection using FuGENE (Promega Corp., Madison, WI, USA). Each transfection included 0.04 µg of the respective *Vsx1* or blank control construct, reporter construct and activator construct, as well as 0.005 µg of the renilla normalizing construct. Twenty-four hours after transfection, the assay was performed using a commercial assay system (Dual-Glo Luciferase; Promega Corp.) and plates were read on a micro-plate reader (Infinite 200 Pro Tecan Life Sciences) according to the manufacturer (Promega Corp.) protocol. Firefly luminescence was normalized to renilla control luminescence. Assays were repeated to an $n = 5$. Data were analyzed using the software GraphPad using a 1-way ANOVA and a multiple comparisons Dunnett's test.

Tissue Preparation for Immunolabeling

Mice were anesthetized with isoflurane and euthanized by cervical dislocation. Eyes were enucleated and were then placed in 4% paraformaldehyde (Cat. # 157-8; Electron Microscopy Science, Hatfield, PA, USA) in 0.15 M phosphate buffer (PB, pH 7.4) and fixed for 20 minutes at room temperature. Eyes were washed in 1X PBS and cryoprotected in 15% sucrose/PB at 4°C for several hours, followed by 30% sucrose/PB at 4°C for several hours and immediately embedded in Tissue-TEK O.C.T. (Cat. # 4583; Sakura Finetek, Torrance, CA, USA) in plastic molds and flash frozen in liquid nitrogen. Sections were cut at 16-µm thickness at −20°C using a cryostat (Leica Biosystems) and mounted on adhesive-coated slides (Newcomer Supply, Middleton, WI, USA, Cat. # 5070). The sections were air dried overnight and stored at −20°C.

Immunolabeling

Prior to immunolabeling slides were immersed in 1% Triton X-100/1X PBS for 30 minutes and then washed in 1X PBS. Primary antibodies: goat anti-GFP (1:500, ab6673; Abcam, Cambridge, UK), chicken anti-GFP (1:500, ab13970; Abcam), sheep anti-Chx10 (1:500, X1180P; Exalpha Biologicals, Shirley, MA, USA), rabbit anti-PKCα (1:10000, P4334; Sigma-Aldrich Corp., St. Louis, MO, USA), rabbit anti-Vsx1 (1:1000; Ed Levine, Vanderbilt, TN, USA), rabbit anti-Recoverin (1:500, AB5585; Chemicon, Tokyo, Japan), goat anti-HSV (1:1000, ab19354; Abcam). Primary antibodies were incubated for either 1 hour at 37°C or 4°C overnight. Secondary antibodies conjugated to AlexaFluor dyes (Invitrogen) were applied at 1:500 dilutions and incubated on tissue for 1 hour at 37°C. All primary and secondary antibodies were prepared in a solution of 1X PBS and 0.1% Triton X-100. After secondary antibody incubation slides were washed in 1X PBS and mounted with Immu-Mount (Cat. # 9990402, Thermo Fisher Scientific, Waltham, MA, USA). Fluorescence confocal microscopy was performed using a confocal microscope (Nikon C2; Nikon Corp., Tokyo, Japan). To quantitate recoverin immunolabeling, a threshold was set for the inner nuclear layer of the retina and retinal bipolar cell somas that were above the set threshold were counted using the cell counting plugin (Cell Counter, https://imagej.nih.gov/ij/plugins/cell-counter.html, in the public domain). Each experiment was repeated at least three times with at least three central retinal regions quantified. Data were analyzed with graphing software (Prism; GraphPad Software, Inc., La Jolla, CA, USA) using a 1-way ANOVA and a multiple comparisons Dunnett's test. Chx10 fluorescence levels were quantitated as described previously.[43]

Electroretinogram Recordings

$VSX1^{P254R/P25R4}$ mice ($n = 5$ females, $n = 3$ males) and littermate control ($n = 8$ females) mice (aged 6–7 weeks) were dark-adapted overnight and prepared under dim red light for ERG recordings. Following anesthesia with a mixture of ketamine (62.5 mg/kg intraperitoneally [IP]) and xylazine (12.5 mg/kg IP) and pupil dilation with 1% tropicamide, animals were placed on a homeothermic blanket to maintain their body temperature at 38°C. Simultaneous bilateral recording was achieved with active gold loop electrodes (placed on each cornea) and subdermal platinum reference electrode (placed behind each eye); a subdermal ground platinum electrode was placed on the mouse's scruff. Light stimulation (10-µs duration flashes), signal amplification (0.3–300 Hz bandpass) and data acquisition were provided by the Espion E^2 system (Diagnosys LLC, Littleton, MA, USA). Scotopic intensity responses consisted of single flash presentations at 19 increasing flash strengths from –5.22 to 2.86 log cd/m^{-2}. Ten minutes after transition from dark to light (30 cd/m^{-2} white light background) adaptation, photopic intensity responses (30 cd/m^{-2} background light) were recorded at 11 increasing flash strengths ranging from –1.6 to 2.9 log cd/m^{-2}. Finally, ON and OFF responses were studied using square and saw tooth (ramp) stimuli. To avoid false duplication, responses from a single eye per animal (yielding the largest saturated a-wave amplitude) were considered.

Using graphing software (GraphPad Software, Inc.), data between the two groups were compared with Kruskall-Wallis, followed (if $P < 0.05$) by the post-hoc two-stage linear step-up procedure of Benjamini, Krieger and Yekutieli,[45] with $Q = 1\%$, which allowed data points to be analyzed individually, without assuming a consistent SD (GraphPad Software, Inc.).

Live Corneal Imaging

Surface Imaging. Intact eyes were enucleated, placed at the bottom of a well filled with 50% SGC5 dye (Biotium Cat # 70057) and oriented under a dissecting scope with the cornea facing up. A round 1.0-mm thickness coverslip was placed over the well. Images were taken using commercial equipment and imaging software (Nikon 4X with numerical aperture [NA] 0.13 and the Nikon EZ-C2; Nikon Corp.). Corneas were imaged with the 488-nm laser and the gain was set to just above saturation for the labeled epithelial cells. Optical *z*-stacks of a 4-µm step were then taken from just above the brightest point of the apex down to the widest diameter, brightest location indicative

of where the cornea meets the sclera. *Z*-stacks were taken for both the right and left eye of three mice of each genotype ranging in age from 6 weeks to 2 months and long-term observation adults that were at least a year and a half in age.

Trans-Corneal Imaging. After surface imaging was complete, eyes were placed in a petri dish containing 1X PBS and a small incision was made at the corneal sclera border with a type 11 surgical blade (Magna Equipment Development Company, Inc.). A small volume (~10 μL) of undiluted SGC5 dye was injected at the incision point. Eyes were placed in the bottom of a well filled with diluted SGC5 dye and were left for a maximum of 5 minutes before they could be imaged. Before imaging, the dish containing the eye was flooded with 1X PBS and oriented with the corneal apex facing up under a dissecting scope. Eyes were imaged with commercial equipment (NA 0.80 W, WD = 3.5 mm, Nikon NIR APO 40X water objective; Nikon Corp.). Five representative optical *z*-stacks with a 2-μm step size were taken across the cornea by first focusing and centering the corneal apex in the field of view. Fiji image analysis software and graphics editing software (Adobe Photoshop CC 2017; Adobe Systems, Inc., San Jose, CA, USA) were used to convert the five optical *z*-stacks into one representative maximum projection image of the cornea. Intensity plots were then generated in Fiji to measure the number of pixels from the brightest top layer (i.e., the epithelial cell layer) and the brightest bottom layer (i.e., the endothelial cell layer) and were converted into corneal thickness. Single measurements were made in both of the most peripheral portions of the reconstructed cornea and two were made in the most central portion. Data were analyzed with graphing software (GraphPad Software, Inc.) using a 1-way ANOVA and a multiple comparison Dunnett's test.

Results

In Vitro Analysis of the VSX1 p.P247R Mutation

To address the pathogenicity of *VSX1* corneal-associated mutations, we first elected to probe *VSX1* p.P247R. In addition to its association with PPCD[31] and keratoconus,[17,18] this mutation has also been associated with an abnormal ERG b-wave,[31] consistent with a role for *Vsx1* in bipolar cell function. *VSX1* p.P247R is also controversial as it has been identified in two unaffected members of a large four generation family in which *VSX1* was excluded as the causative gene in a large PPCD1/chromosome 20 family.[34] Regardless, the p.P247R change is compelling: first, the amino acid change of a proline (associated with introducing bends in the secondary structure) to arginine (charged residue) is predicted to be highly pathogenic by the prediction tool PredictSNP[46]; second, p.P247 is located within the CVC domain, a highly conserved domain directly adjacent to the homeodomain that is found exclusively in all Prd-L:CVC sequences; third, p.P247 is located at a position within the CVC domain that conserved in all vertebrate, fly, and nematode Prd-L:CVC homologues (Fig. 1), suggesting it is critical for protein function.

To determine whether the *VSX1* p.P247R change alters VSX1 transcriptional activity, we developed a luciferase reporter repressor assay based on a previous study.[47] Our study utilized the corresponding orthologous mutation, p.P254R, in mouse *Vsx1* as we were ultimately interested in examining this mutation in the context of the mouse, in vivo. The reporter construct encodes five upstream activator sequences (UAS) that mediate transcriptional activation driven by a cotransfected HSF-Gal4 activator, as well as four P3 homeodomain binding sites that interact with cotransfected VSX1 (see Fig. 4A). As previously shown,[47] wild-type VSX1 functions as a robust transcriptional repressor in vitro (see Fig. 4B). Mouse VSX1 p.P254R, showed a 2-fold increase in repressor activity compared to wild-type VSX1. This change in activity was observed in both HSV-tagged and untagged versions of VSX1 and in experiments using VP16-GAL4 as an alternative activator (data not shown). No differences in protein expression or cellular localization were observed between wild-type and p.P254R VSX1 by Western blotting or by immunohistochemistry, respectively (Fig. 2C; Supplementary Figs. S1, S2), suggesting that this mutation leads to enhanced VSX1 transcriptional repressor activity.

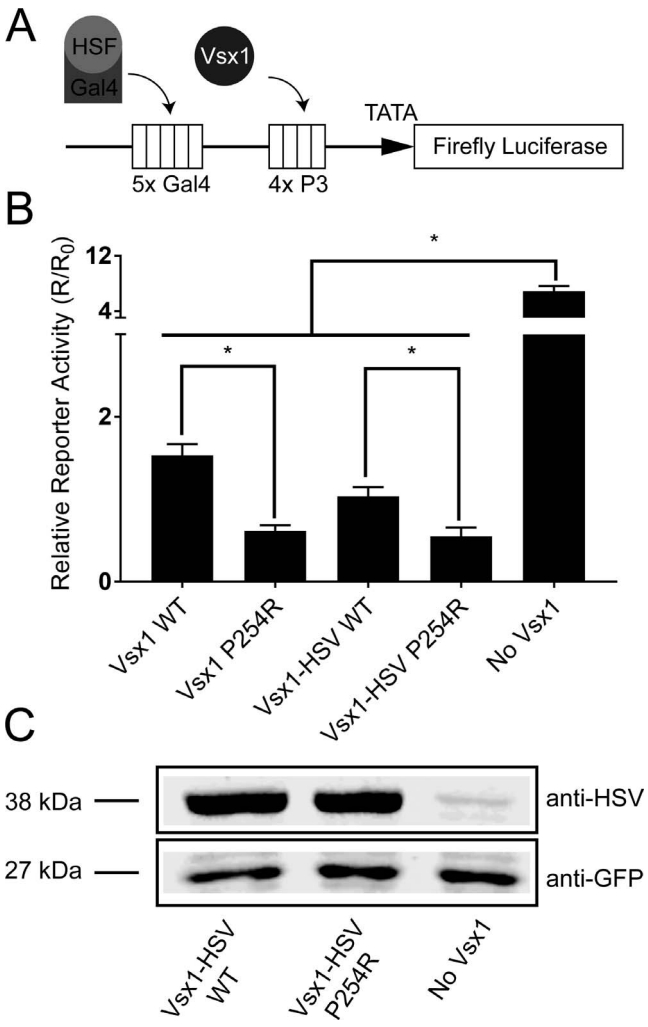

Figure 2. Mouse VSX1 p.P254R exhibits enhanced transcriptional repressor activity. (**A**) Overview of the 5xGal4-4xP3-TATA-Luciferase reporter VSX1 transcriptional repressor assay. (**B**) Relative reporter expression, normalized to a renilla control construct, in vitro. Two-tailed *t*-test revealed a significant difference between p.P254R and WT VSX1 with a *P* value of 0.004 ($n = 11$). (**C**) Western blot of lysates from HEK 293T transfected with HSV-tagged wild type VSX1 or mouse VSX1 p.P254R. GFP was co-transfected as a loading control.

Analysis of the Vsx1 P254R Mutant

Generation of the Vsx1 P254R Mutant. To examine whether *VSX1* p.P247R is pathogenic in vivo, we utilized CRISPR-Cas9 gene editing to introduce the corresponding mouse change, p.P254R, into mouse *Vsx1* (Fig. 3). A guide RNA targeting the endogenous *Vsx1* gene and introducing the p.P254R change (CCA to AGG) also introduced a silent mutation in the adjacent leucine residue to create a BspE1

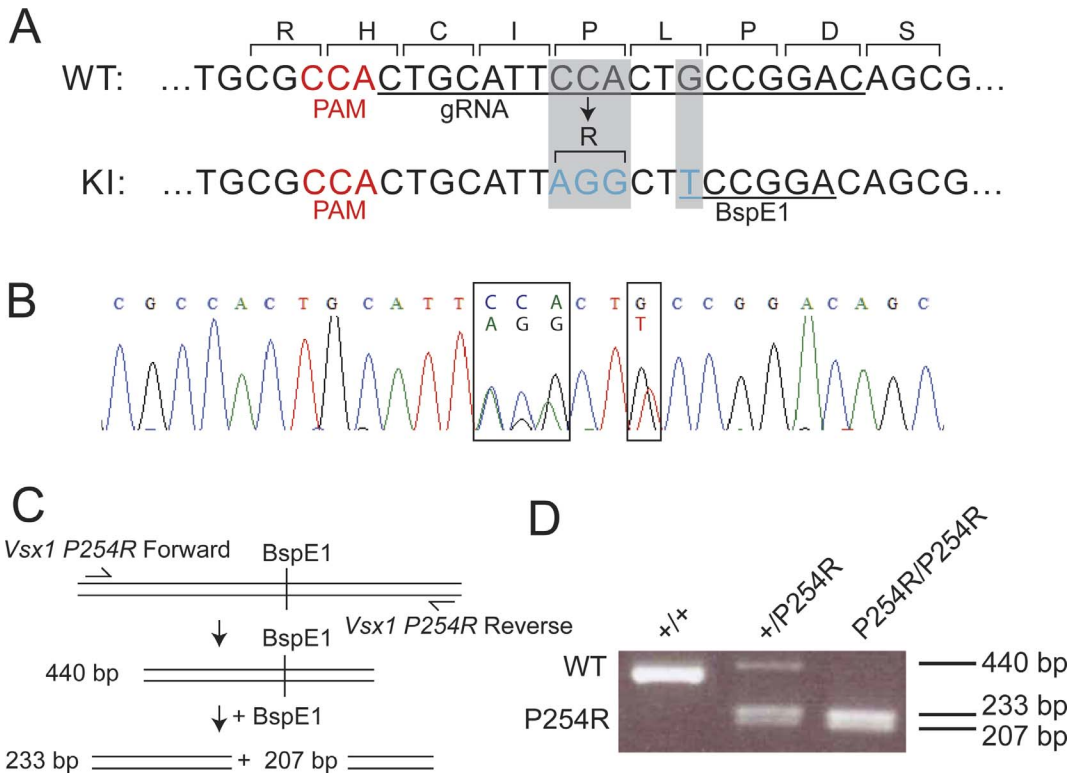

Figure 3. Generation of a mouse model for human *VSX1* p.P247R. (**A**) CRISPR-Cas9 strategy for directing the proline 254-to-arginine change (donor strand not shown). The guide RNA (gRNA) is underlined. A silent mutation shown in blue that introduces a BspE1 restriction site for genotyping purposes. (**B**). Chromatogram showing sequence of a heterozygous mouse carrying both the missense and silent mutations. (**C**). Genotyping strategy for $Vsx1^{P254R}$ mouse line. (**D**) Representative gel showing the PCR and BspE1 digest products.

restriction site to facilitate genotyping (Figs. 3B–D). Out of four potential founders, two independent lines carrying the desired mutations were identified and the *Vsx1* coding regions sequenced and found not to have any off-target mutations. Mice heterozygous or homozygous for $Vsx1^{P254R}$ were healthy and viable and did not show any gross morphologic ocular abnormalities compared to wild-type mice.

Morphometric Analysis of Unfixed Cornea. To determine whether $Vsx1^{P254}$ mice exhibit any corneal abnormalities, hematoxylin and eosin staining of paraffin-embedded sections was performed (Figs. 4A–C). We did not observe any of the hallmark features of PPCD, such as endothelial cell multilayering in $Vsx1^{P254R/P254R}$ mutants, nor did we observe any obvious change in corneal thickness that is associated with keratoconus. However, as conventional histologic preparation of the cornea is prone to tissue shrinkage, cracking, and loss of morphology, it was not ideal for obtaining reliable quantitative measurements of corneal metrics. To overcome this, we developed a two-step protocol for imaging the unfixed live cornea. First, freshly dissected whole eyes were placed in a solution of the fluorescent lipophilic dye, SGC5. Immediate uptake of the dye onto the corneal outer surface enabled confocal imaging of the entire corneal surface, *z*-plane maximum projection to obtain a cross-section of the cornea (e.g., Figs. 4G–I) and subsequent measurement of curvature. As SGC5 does not penetrate the corneal layers under these circumstances, we found that by making a single small incision in the limbal region, injected dye was rapidly taken up by all corneal cell layers. This allowed for high resolution, confocal imaging through all of the corneal layers, z-plane cross-sectional maximum intensity projections and measurement of corneal thickness.

Using this imaging approach, we examined the corneas of wild-type and *P254R* homozygous mice at two time points, 6 to 10 weeks and >1 year of age. We included older time points as PPCD and keratoconus are progressive diseases and often present later in life.[1,11] As with our hematoxylin histology data, we did not observe any multilayering of the corneal endothelium in $Vsx1^{P254R/P254R}$ mutants (Figs. 4D–F). Similarly, we did not observe any change in either corneal thickness (Figs. 4J, 4K) or curvature (Figs. 4L, 4M) in the *P254R* mutants compared to wild-type. Using this imaging approach, we also examined the corneas of *Vsx1*-null mice. We also did not observe any significant changes in corneal thickness or curvature (Figs 4J, 4L, 4M). Together, these data show that in mouse, *Vsx1* p.P254R does not lead to any measurable changes in corneal morphology.

Retinal Analysis. As *Vsx1* is required in mice for the terminal differentiation of a subset of bipolar interneurons,[40–43] we next asked whether *Vsx1 P254R* mutant mice exhibit any retinal defects. Immunolabeling for VSX1 showed normal distribution and nuclear localization in the bipolar cell region of the inner nuclear layer (Figs. 5A–C). Immunolabeling for the retinal bipolar cell markers recoverin (Figs. 5D–F) and Chx10/Vsx2 (Figs. G–I), which are downregulated[40] and upregulated,[43] respectively, in *Vsx1*-null mice, was unaffected in $Vsx1^{P254R/P254R}$ mutants (Figs. 5M, 5N). These findings indicate that for at least two molecular markers, the $Vsx1^{P254R/P254R}$ retina is indistinguishable from wild-type and does not lead to the same defects observed in *Vsx1*-null mice.

Although we did not observe abnormal recoverin or Chx10 immunostaining similar to that observed in the *Vsx1* null-mouse,[40,41,43] it is possible that the p.P254R mutation results in a unique retinal phenotype given that the *Vsx1*

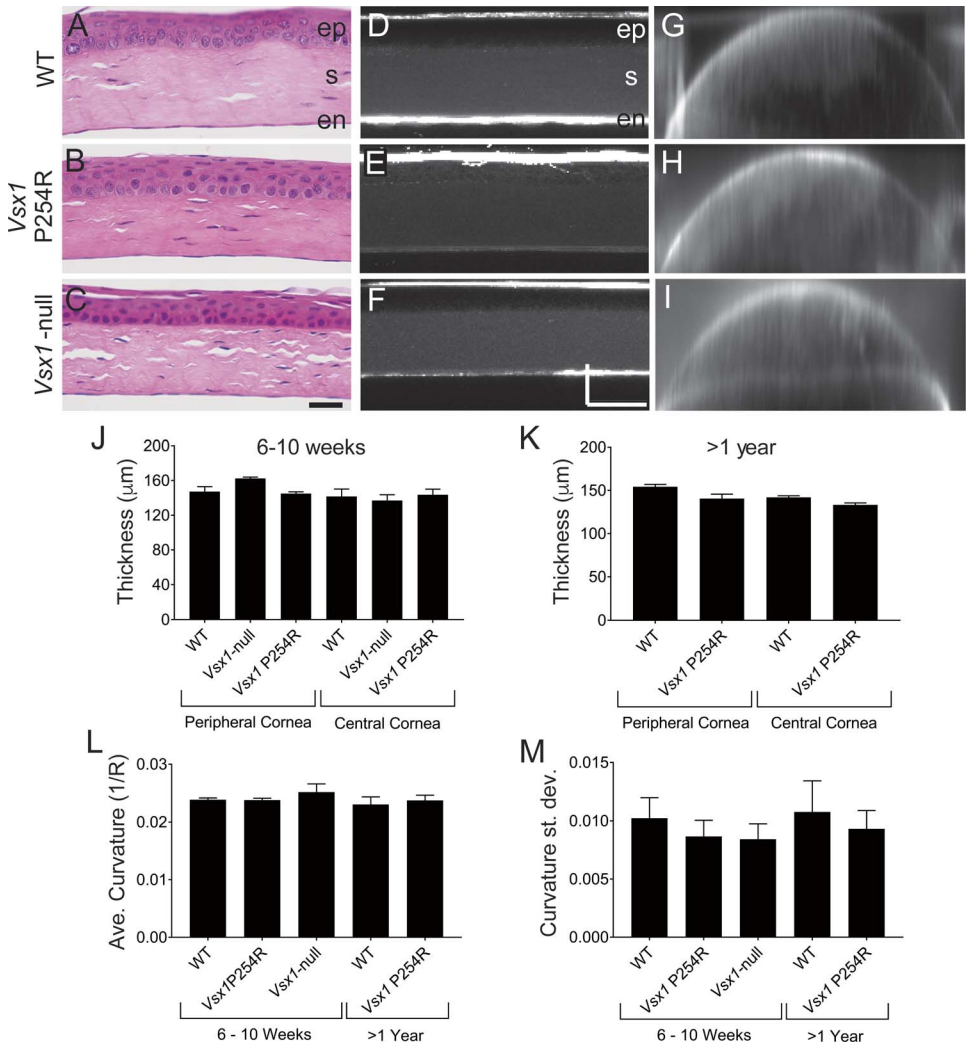

Figure 4. Absence of histologic and morphometric abnormalities in *Vsx1*$^{P254R/P254R}$ mice. (**A–C**) Hematoxylin and eosin staining of paraffin-embedded mouse corneal sections ranging in age from 6 to 10 weeks. en, endothelium; ep, epithelium; s, stroma. *Scale bar* in (**C**) = 50 μm. (**D–I**) Confocal imaging of SGC5 fluorescence. 50 μm maximum *x-z* projections of the most central stack taken through the central apex of unfixed corneas injected with SGC5 dye. *Scale bar* in (**F**) = 50 μm (*z*) by 25 μm (*x*). Average intensity *x-z* projection of uninjected eyes bathed in SGC5. (**J**, **K**) Graph showing thickness of central cornea measured from *z-x* projections of SGC5 dye injected eyes between the ages of 6 and 10 weeks (**J**) and 1 year or older (**K**). 1-way ANOVA revealed no significant differences between genotypes ($n = 3$ animals per genotype). Graph showing average curvature (**L**) and curvature standard deviation (**M**) calculated from average intensity *x-z* projection of uninjected eyes bathed in SGC5.

p.P254R mutation has a gain-of-function (Fig. 2) rather than loss-of-function phenotype. We therefore performed ERG to determine whether retina visual signaling was altered in *Vsx1*$^{P254R/P254R}$ mice. Dark-adapted (Figs. 6A–E) and light-adapted (Fig. 6F–J) responses showed subtle changes in *P254R* mutants compared to wild-type controls. Mixed a-wave amplitudes (reflecting the light-driven stoppage of dark-current from rods and cones) were overall higher in mutants; post-hoc analysis did not pick up any effects specific to flash strength (Fig. 6A). Photopic cone b-waves (reflecting the light-driven postsynaptic depolarization of ON cone bipolar cells) had higher amplitudes, specifically for the strongest flash strengths. However, another test related to cone bipolar cells, the flicker ERG, did not show differences between groups (Fig. 6K).

With the aim of discriminating between ON and OFF cone bipolar function, we presented the mice with square wave and saw tooth stimuli (Figs. 6L–O) and labeled the components obtained as previously proposed.[48] The negative deflections (negative OFF), elicited by square wave stimulus offset (Fig. 6L) are in agreement with the synchronous occurrence of a negative component originating from ON cone bipolar cells. Impairment of ON responses, such as in *nob* mice[49] or following intravitreal (6)-cis-piperidine-2,3-dicarboxilic acid,[50,51] allows recording positive ERG responses from OFF bipolar cells (d-wave) in mice. The exacerbation of the negative OFF response in *Vsx1*$^{P254R/P254R}$ mice (black arrow in Figs. 6L, 6M, 6O), alongside higher photopic b-wave amplitudes (Fig. 6H), point toward an imbalance favoring ON as opposed to OFF cone bipolar cell visual responsiveness to whole field stimuli. Together, our findings indicate that while the *Vsx1* p.P254R mutation does not cause a molecular defect resembling that observed in *Vsx1*-null mice, it does lead to more prominent ON as opposed to OFF panretinal responsiveness. Whether our findings of increased mixed a-wave amplitudes (Fig. 6A) might be evidence for a direct effect of the *Vsx1* p.P254R mutation on photoreceptor physiology itself remains to be elucidated.

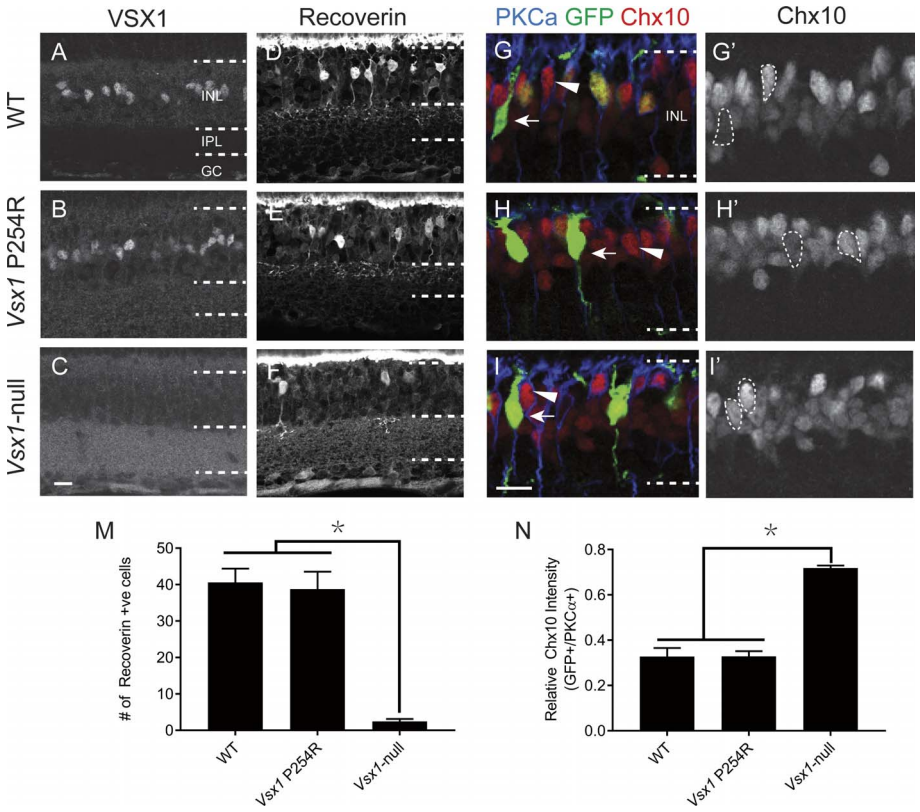

Figure 5. Recoverin and Chx10 immunolabeling in the *Vsx1*$^{P254R/P254R}$ retina is indistinguishable from wild-type and does not phenocopy the *Vsx1*-null mutant. Immunofluorescence labeling for Vsx1 (**A–C**), recoverin (**D–F**) and Chx10 (**G–I**). Immunolabeling in the *Vsx1 P254R* homozygous retina is indistinguishable from wild-type controls and does not exhibit the loss of recoverin positive cells (**M**) or the upregulation of Chx10 in α-gustducin:GFP^{+} Type 7 ON cone bipolar cells (**N**) that is observed in *Vsx1*-null mice.

In Vitro Analysis of Other VSX1 Missense Mutations

While the *Vsx1* p.P254R mutation did not lead to an observable phenotype in the mouse, it did alter VSX1 transcriptional repressor activity, in vitro. We were therefore interested in determining whether other *VSX1* mutations associated with PPCD and keratoconus altered VSX1 transcriptional repressor activity. We focused on five *VSX1* mutations based on their position and invariability (in vertebrate, fly and nematodes *Vsx* homologues, see Fig. 1 and Table 2) within the homeodomain/CVC domain. Four of the mutations we tested (p.R173W, p.Q182H, p.G246R and p.H251R), trended toward enhanced repressor activity compared to wild-type VSX1 (similar to p.P254R), although not reaching statistical significance. One mutation, p.A263S, had comparable activity to wildtype VSX1 (Fig. 7B). Western blotting (Supplementary Fig. S1) and immunocytochemistry (Supplementary Fig. S2) showed that none of the mutations affected protein expression or nuclear localization. These findings indicate that most PPCD- and keratoconus-associated VSX1 mutations that change highly conserved amino acid residues alter VSX1 transcriptional activity in vitro.

Discussion

Many publications have described *VSX1* mutations associated with PPCD and/or keratoconus (Table 1); however, there is uncertainty as to the role, if any, *VSX1* plays in these corneal diseases. Compounding this uncertainty is the lack of experimental work to examine the pathogenicity of the mutations that have been identified. Here, we have addressed this issue through in vitro and in vivo experiments in mouse. Our study is the first to generate a mouse *Vsx1* mutant harboring a mutation associated with human corneal disease. Despite altering transcriptional repressor activity in vitro, *Vsx1* p.P254R (the mouse mutation corresponding to human *VSX1* p.P247R) did not lead to pathogenic changes in either the heterozygous (data not shown) or homozygous mouse cornea, although it did lead to mild retinal visual signaling defects.

While we cannot conclude from our study that *VSX1* does not play a role in human PPCD, there is compelling evidence against it playing a major role. First, *Vsx1/VSX1* expression has not been detected in either the mouse (mRNA, protein, reporter gene),[39,52] or human (mRNA)[31] cornea. Second, several *VSX1* mutations associated with PPCD, including p.P247R, have also been detected in unaffected individuals and in some cases did not segregate with affected individuals in some familial studies.[18,20,24,26,29–31,33–36] Third, chromosome 20p mapping studies have now identified *OVOL2* as the disease-causing gene for PPCD1.[34,37,38] Mutations in the *OVOL2* promoter region lead to ectopic OVOL2 expression in the corneal endothelium, where it functions as a transcriptional repressor of ZEB1,[38,53,54] a transcription factor that is essential for normal corneal endothelial and keratocyte development and is mutated in PPCD3 (MIM: 609141).[55] Interestingly, a similar mechanism whereby *ZEB1* is repressed by ectopic *GRHL2* expression in the corneal endothelium, is thought to underlie PPCD4 (8q22.3–q24.12).[56]

The role of *VSX1* in keratoconus is more unclear. While two previous studies identified *VSX1* p.P247R (the main focus of our current study) in individuals with keratoconus and not in control subjects,[17,18] p.P247R has also been identified in the

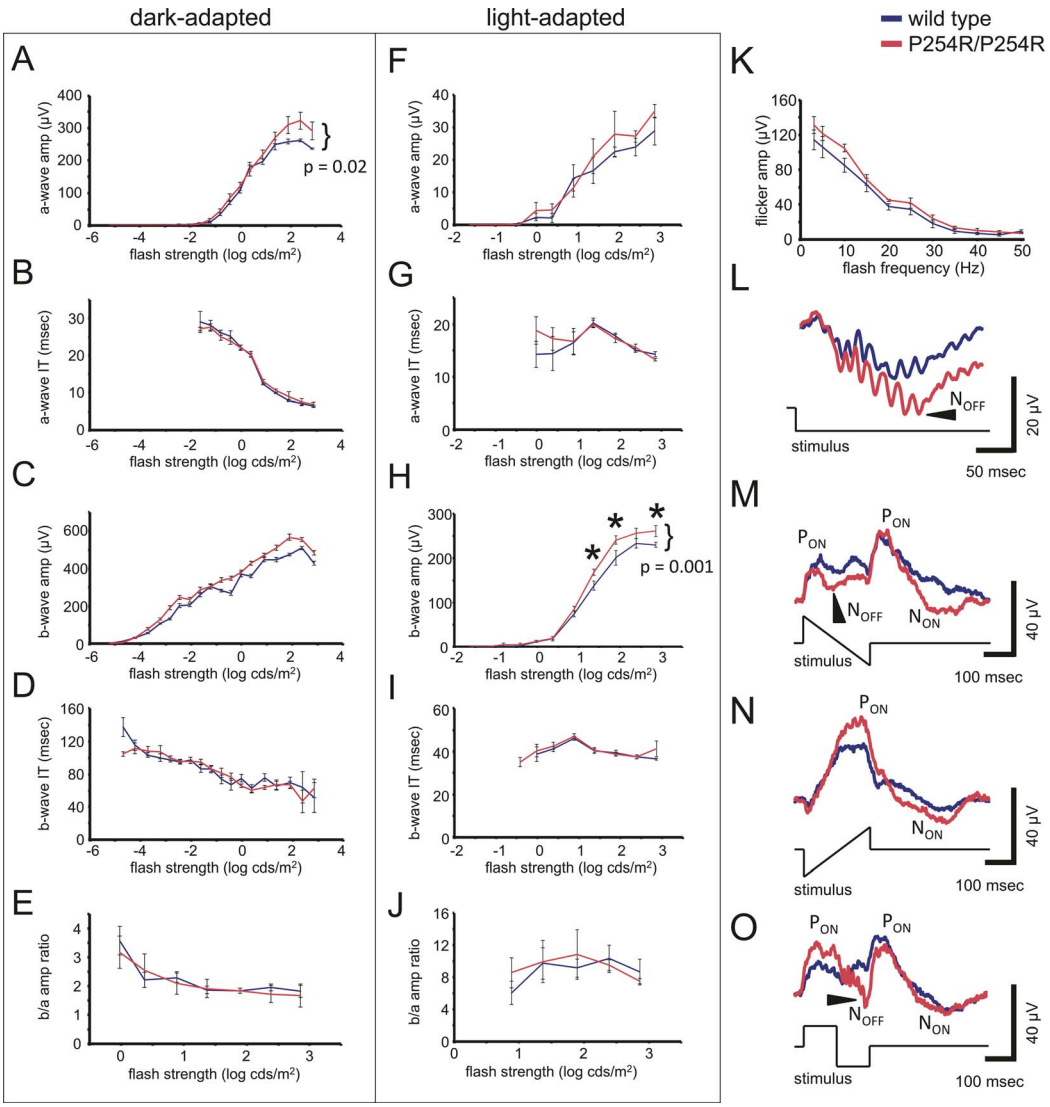

Figure 6. Electroretinography reveals imbalances favoring ON versus OFF visual signal processing in the *Vsx1*$^{P254R/P254R}$ retina. Components of the dark-adapted ERG higher a-wave amplitudes in *Vsx1*$^{P254R/P254R}$ mice compared to wild-type control: (**A**) a-wave amplitude, (**B**) a-wave implicit time, (**C**) b-wave amplitude, (**D**) b-wave implicit time, (**E**) b/a ratio. Components of the light-adapted ERG showed higher b-wave amplitudes in *Vsx1*$^{P254R/P254R}$ mice compared to wild-type control: (**F**) a-wave amplitude, (**G**) a-wave implicit time, (**H**) b-wave amplitude, (**I**) b-wave implicit time, (**J**) b/a ratio, (**K**) flicker ERG. Exacerbated negative response to square wave stimulus offset (**L** and **O**, *arrowheads*) and downward saw tooth stimuli (**M**, *arrowhead*) were observed. In addition, positive ON responses were more prominent following upward saw tooth (**N**) and square wave stimulus onset (**O**). Traces in (**L**–**O**) represent averaged responses from $n = 6$ animals per genotype. P_{ON}, positive ON response; N_{ON}, negative ON response; N_{OFF} negative OFF response. The *right curly bracket* indicates significant difference between curves, while *asterisks* indicate data points with post-hoc significance at $P < 0.05$.

control population.[34] Other studies, which have associated *VSX1* mutations in individuals with keratoconus also identified the same mutations in the control population.[18,20,26,28,31,32] In the current study, we did not observe any of the hallmark signs of keratoconus in *Vsx1*^{P254R} mutant mice. Together, these observations make it reasonable to conclude that *VSX1* mutations do not have a strong causal role in keratoconus. However, similar to what has previously been concluded,[18] we cannot completely exclude a role for *VSX1* in keratoconus. "Non-affected" individuals with *VSX1* mutations could potentially have subtle abnormalities that lie at the threshold of the disease spectrum, or the mutation may be incompletely penetrant in one individual and pathogenic in another due to the requirement of additional factors in order to reach a disease state.[18] In addition, while *Vsx1/VSX1* expression has not been detected in either the mouse or human cornea,[31,39] it could potentially play a non-cell autonomous role in keratoconus. For instance, retinal dysfunction resulting from mutations in human *VSX1*, may have long term secondary effects on corneal morphology and homeostasis that cannot be observed in a mouse model. Another intriguing possibility comes from our observation that *Vsx1* mRNA can be detected in the mouse trigeminal ganglion (data not shown). Sensory neurons from the ophthalmic branch of the trigeminal ganglion project to the corneal stroma and epithelium, and in addition to being vital for detecting harmful stimuli, these neurons are also believed to provide chemical feedback onto these corneal layers.[57,58]

Although the *Vsx1* p.P254R mutation did not lead to any major dark- or light-adapted visual signaling defects, there were abnormalities in the mutant OFF response as assayed by ERG. This was one area where a phenotype had been anticipated given that the role for *Vsx1* in visual signaling which has been

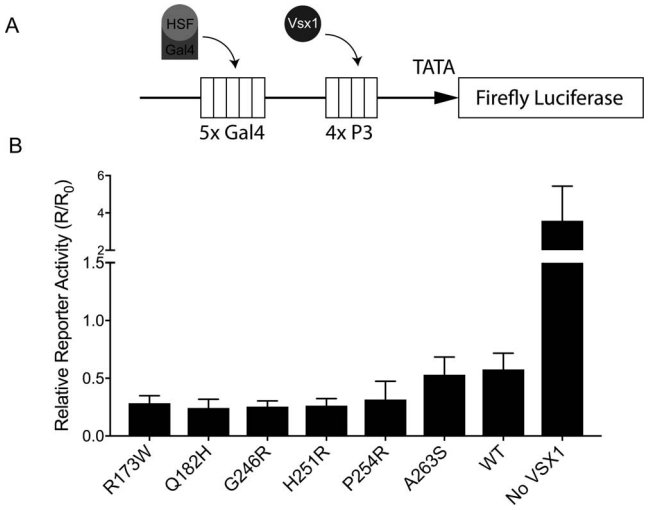

Figure 7. Perturbed transcriptional repressor activity of disease-associated Vsx1 missense mutations in HEK 293T cells. (**A**) Overview of the 5xGal4-4xP3-TATA-Luciferase reporter VSX1 transcriptional repressor assay. (**B**) Relative luciferase reporter expression, normalized to a co-transfected renilla control construct in HEK 293T cells ($n = 5$). $^{*}P < 0.002$ compared to wild-type Vsx1.

well described in mice.[40,41,43] Humans with *VSX1* mutations have also been found to have an abnormal ERG, consistent with an inner retinal defect.[24,29,31] Again, there are inconsistencies in phenotype: in one study a single individual with the p.P247R mutation (and no corneal defect) had an abnormal ERG,[31] while in another study two individuals with keratoconus and also carrying p.P247R had a normal ERG.[17] As only a few studies have performed ERG studies in individuals carrying *VSX1* mutations, it is difficult to predict how *VSX1* mutations affect human vision, especially given the mild nature of the defects observed in *Vsx1* mouse mutants. However, as *Vsx1* function in ON cone bipolar cells is required for the proper retinal directional selectivity,[43] one could argue that this type of circuit-specific function could profoundly impact vision, even though most of the retina is intact.

Prd-L:CVC genes encodes homeodomain transcription factors (VSX1 and VSX2/CHX10 in vertebrates) and have previously been shown to possess transcriptional repressor activity.[47] Our study confirms this for VSX1 and is the first to show that mutations within the VSX1 CVC domain (p.G246R, p.H251R and p.P254R) alter transcriptional activity by specifically enhancing repressor activity. As these changes do not alter protein expression or subcellular localization, it suggests that the CVC domain may influence DNA binding or may be involved in protein-protein interactions that mediate repression. Interestingly, human VSX1 p.R166W and its corresponding mouse mutation, VSX1 p.R173W, exhibit different functional phenotypes. Human VSX1 p.R166W has previously been shown to inhibit VSX1 repressor activity,[47] while in our study, mouse VSX1 p.R173W enhanced repressor activity. This difference may reflect functional differences between mouse and human VSX1 stemming from the relatively low level of sequence conservation between these orthologues.[40] From an evolutionary standpoint, it would be interesting to compare the transcriptional activity, protein-protein interactions, and DNA binding capacity of mouse and human *VSX1* orthologues. This also points out a potential caveat to using mouse as a model for studying *VSX1*-associated ocular disease.

If *VSX1* is not playing a major role in PPCD and keratoconus, why has it been implicated with these diseases in so many studies? The simplest possibility is that these are nonpathogenic naturally occurring variants. When assessing a variant for a causative role in a dominant Mendelian disease, like PPCD, the general, albeit oversimplified rule is that the frequency of a variant in a reference sample should not exceed disease prevalence.[59] Mining of the gnomAD database (r2.0.2) revealed that the allele frequency of the six *VSX1* mutations examined in our study (Table 1) ranges between 2.63×10^{-3} and 4.06×10^{-6}. Although the disease prevalence of PPCD has not been well described, one study estimated what was considered by the authors to be a high prevalence of PPCD of 1:100,000 in the Czech Republic.[60] Assuming that PPCD is just as or less prevalent in other populations, the allele frequency of *VSX1* variant p.H244R (2.63×10^{-3}) makes it about 100 times more prevalent than PPCD1, and therefore more likely to be nonpathogenic. p.247R and p.A256S, on the other hand have an allele frequency about an order of magnitude greater than the disease prevalence, while p.R166W, p.Q175H and p.G239R have an allele frequency that is in a similar range or less than the disease prevalence, thus any definitive conclusions on pathogenicity based of this criterion alone are not possible. It is also difficult to compare *VSX1* allele frequency with keratoconus as this disease does not appear to have strong evidence supporting a simple Mendelian mode of inheritance and instead appears to be complex. Finally, it is important to note that there are several amino acid residues in the homeodomain and CVC domain, including some of the mutated residues examined in our current study, that are conserved across all vertebrate and invertebrate *VSX* orthologues. This indicates that these amino acids are critical to some function of *VSX1*. We suggest that in humans, as in mouse, *VSX1* is primarily required for fine-tuning optimal retinal function. While it is clear that *VSX1* does not play a causative role in PPCD1, we cannot not rule out, at this time, a role for *VSX1* in keratoconus, although it likely does not play a major causative role.

Acknowledgments

The authors thank R. Bremner for 5xGal4-4xP3-TATA-luciferase and pBXG6-HSF1 plasmids. Supported by operating grants to RLC from the Canadian Institute of Health Research and National Sciences and Engineering Research Council of Canada.

Disclosure: **A.M. Litke**, None; **S. Samuelson**, None; **K.R. Delaney**, None; **Y. Sauvé**, None; **R.L. Chow**, None

References

1. Weiss JS, Ulrik Møller H, Aldave AJ, et al. IC3D Classification of Corneal Dystrophies-Edition 2. *Cornea*. 2015;34:117–159.
2. Rodrigues M, Sun J, Krachmer J, Newsome D. Epithelialization of the corneal endothelium in posterior polymorphous dystrophy. *Invest Ophthalmol Vis Sci*. 1980;19:832–835.
3. de Felice GP, Braidotti P, Viale G, Bergamini F, Vinciguerra P. Posterior polymorphous dystrophy of the cornea. *Graefes Arch Clin Exp Ophthalmol*. 1985;223:265–271.
4. Lam HY, Wiggs JL, Jurkunas UV. Unusual presentation of presumed posterior polymorphous dystrophy associated with iris heterochromia, band keratopathy, and keratoconus. *Cornea*. 2010;29:1180–1185.
5. Cremona FA, Ghosheh FR, Rapuano CJ, et al. Keratoconus associated with other corneal dystrophies. *Cornea*. 2009;28:127–135.
6. Driver PJ, Reed JW, Davis RM. Familial cases of keratoconus associated with posterior polymorphous dystrophy. *Am J Ophthalmol*. 1994;118:256–257.

7. Blair SD, Seabrooks D, Shields WJ, Pillai S, Cavanagh HD. Bilateral progressive essential iris atrophy and keratoconus with coincident features of posterior polymorphous dystrophy: a case report and proposed pathogenesis. *Cornea*. 1992; 11:255–261.
8. Bechara SJ, Grossniklaus HE, Waring GO, Wells JA. Keratoconus associated with posterior polymorphous dystrophy. *Am J Ophthalmol*. 1991;112:729–731.
9. Weissman BA, Ehrlich M, Levenson JE, Pettit TH. Four cases of keratoconus and posterior polymorphous corneal dystrophy. *Optom Vis Sci*. 1989;66:243–246.
10. Gasset AR, Zimmerman TJ. Posterior polymorphous dystrophy associated with keratoconus. *Am J Ophthalmol*. 1974;78: 535–537.
11. Krachmer JH, Feder RS, Belin MW. Keratoconus and related noninflammatory corneal thinning disorders. *Surv Ophthalmol*. 1984;28:293–322.
12. Edwards M, McGhee CN, Dean S. The genetics of keratoconus. *Clin Exp Ophthalmol*. 2001;29:345–351.
13. Aldave AJ, Yellore VS, Salem AK, et al. No VSX1 gene mutations associated with keratoconus. *Invest Opthalmol Vis Sci*. 2006;47:2820.
14. Valgaeren H, Koppen C, Van Camp G. A new perspective on the genetics of keratoconus: why have we not been more successful? *Ophthalmic Genet*. 2018;39:158–174.
15. Chang H-YP, Chodosh J. The genetics of keratoconus. *Semin Ophthalmol*. 2013;28:275–280.
16. Héon E, Mathers WD, Alward WL, et al. Linkage of posterior polymorphous corneal dystrophy to 20q11. *Hum Mol Genet*. 1995;4:485–488.
17. Bisceglia L, Ciaschetti M, De Bonis P, et al. VSX1 Mutational analysis in a series of italian patients affected by keratoconus: detection of a novel mutation. *Invest Opthalmol Vis Sci*. 2005;46:39–45.
18. De Bonis P, Laborante A, Pizzicoli C, et al. Mutational screening of VSX1, SPARC, SOD1, LOX, and TIMP3 in keratoconus. 2011;17:2482–2494.
19. Mok J-W, Baek S-J, Joo C-K. VSX1 gene variants are associated with keratoconus in unrelated Korean patients. *J Hum Genet*. 2008;53:842–849.
20. Tang YG, Picornell Y, Su X, Li X, Yang H, Rabinowitz YS. Three VSX1 gene mutations, L159M, R166W, and H244R, are not associated with keratoconus. *Cornea*. 2008;27:189–192.
21. Saee-Rad S, Hashemi H, Miraftab M, et al. Mutation analysis of VSX1 and SOD1 in Iranian patients with keratoconus. *Mol Vis*. 2011;17:3128–3136.
22. Paliwal P, Tandon R, Dube D, Kaur P, Sharma A. Familial segregation of a VSX1 mutation adds a new dimension to its role in the causation of keratoconus. *Mol Vis*. 2011;17:481–485.
23. Tanwar M, Kumar M, Nayak B, et al. VSX1 gene analysis in keratoconus. *Mol Vis*. 2010;16:2395–2401.
24. Valleix S, Nedelec B, Rigaudiere F, et al. H244R VSX1 Is associated with selective cone on bipolar cell dysfunction and macular degeneration in a PPCD family. *Invest Opthalmol Vis Sci*. 2006;47:48–54.
25. Shetty R, Nuijts RMMA, Nanaiah SG, et al. Two novel missense substitutions in the VSX1 gene: clinical and genetic analysis of families with Keratoconus from India. *BMC Med Genet*. 2015; 16:33.
26. Jeoung JW, Kim MK, Park SS, et al. VSX1 gene and keratoconus: genetic analysis in Korean patients. *Cornea*. 2012;31:746–750.
27. Vincent AL, Jordan C, Sheck L, Niederer R, Patel DV, McGhee CNJ. Screening the visual system homeobox 1 gene in keratoconus and posterior polymorphous dystrophy cohorts identifies a novel variant. *Mol Vis*. 2013;19:852–860.
28. Liskova P, Dudakova L, Krepelova A, Klema J, Hysi PG. Replication of SNP associations with keratoconus in a Czech cohort. Novelli G, ed. *PLoS One*. 2017;12:e0172365.
29. Mintz-Hittner HA, Semina EV, Frishman LJ, Prager TC, Murray JC. VSX1 (RINX) mutation with craniofacial anomalies, empty sella, corneal endothelial changes, and abnormal retinal and auditory bipolar cells. *Ophthalmology*. 2004;111:828–836.
30. Aldave AJ, Yellore VS, Principe AH, et al. Candidate gene screening for posterior polymorphous dystrophy. *Cornea*. 2005;24:151–155.
31. Heon E, Greenberg A, Kopp KK, et al. VSX1: a gene for posterior polymorphous dystrophy and keratoconus. *Hum Mol Genet*. 2002;11:1029–1036.
32. Eran P, Almogit A, David Z, et al. The D144E Substitution in the VSX1Gene: A non-pathogenic variant or a disease causing mutation? *Ophthalmic Genet*. 2008;29:53–59.
33. Dash DP, George S, O'Prey D, et al. Mutational screening of VSX1 in keratoconus patients from the European population. *Eye (Lond)*. 2010;24:1085–1092.
34. Gwilliam R, Liskova P, Filipec M, et al. Posterior polymorphous corneal dystrophy in Czech families maps to chromosome 20 and excludes the VSX1 gene. *Invest Ophthalmol Vis Sci*. 2005;46:4480–4484.
35. Dehkordi FA, Rashki A, Bagheri N, et al. Study of VSX1 mutations in patients with keratoconus in southwest Iran using PCR-single-strand conformation polymorphism/heteroduplex analysis and sequencing method. *Acta Cytol*. 2013;57: 646–651.
36. Liskova P, Ebenezer ND, Hysi PG, et al. Molecular analysis of the VSX1 gene in familial keratoconus. *Mol Vis*. 2007;13: 1887–1891.
37. Chung DD, Frausto RF, Cervantes AE, et al. Confirmation of the OVOL2 promoter mutation c.-307T>C in posterior polymorphous corneal dystrophy 1. *PLoS One*. 2017;12: e0169215.
38. Davidson AE, Liskova P, Evans CJ, et al. Autosomal-dominant corneal endothelial dystrophies CHED1 and PPCD1 are allelic disorders caused by non-coding mutations in the promoter of OVOL2. *Am J Hum Genet*. 2016;98:75–89.
39. Watson T, Chow RL. Absence of Vsx1 expression in the normal and damaged mouse cornea. *Mol Vis*. 2011;17:737–744.
40. Chow RL, Volgyi B, Szilard RK, et al. Control of late off-center cone bipolar cell differentiation and visual signaling by the homeobox gene Vsx1. *Proc Natl Acad Sci U S A*. 2004;101: 1754–1759.
41. Ohtoshi A, Wang SW, Maeda H, et al. Regulation of retinal cone bipolar cell differentiation and photopic vision by the CVC homeobox gene Vsx1. *Curr Biol*. 2004;14:530–536.
42. Shi Z, Jervis D, Nickerson PEB, Chow RL. Requirement for the paired-like homeodomain transcription factor VSX1 in type 3a mouse retinal bipolar cell terminal differentiation. *J Comp Neurol*. 2012;520:117–129.
43. Shi Z, Trenholm S, Zhu M, et al. Vsx1 regulates terminal differentiation of type 7 ON bipolar cells. *J Neurosci*. 2011;31: 13118–13127.
44. Huang L, Shanker YG, Dubauskaite J, et al. Gγ13 colocalizes with gustducin in taste receptor cells and mediates IP3 responses to bitter denatonium. *Nat Neurosci*. 1999;2:1055–1062.
45. Benjamini Y, Krieger AM, Yekutieli D. Adaptive linear step-up procedures that control the false discovery rate. *Biometrika*. 2006;93:491–507.
46. Bendl J, Stourac J, Salanda O, et al. PredictSNP: robust and accurate consensus classifier for prediction of disease-related mutations. *PLoS Comput Biol*. 2014;10:e1003440.

Investigative Ophthalmology & Visual Science

47. Dorval KM, Bobechko BP, Ahmad KF, Bremner R. Transcriptional activity of the paired-like homeodomain proteins CHX10 and VSX1. *J Biol Chem*. 2005;280:10100–10108.
48. Tsai TI, Barboni MTS, Nagy BV, et al. Asymmetrical functional deficits of ON and OFF retinal processing in the mdx 3Cv mouse model of duchenne muscular dystrophy. *Invest Opthalmol Vis Sci*. 2016;57:5788–5798.
49. Shirato S, Maeda H, Miura G, Frishman LJ. Postreceptoral contributions to the light-adapted ERG of mice lacking b-waves. *Exp Eye Res*. 2008;86:914–928.
50. Naarendorp F, Williams GE. The d-wave of the rod electroretinogram of rat originates in the cone pathway. *Vis Neurosci*. 1999;16:91–105.
51. Xu L, Ball SL, Alexander KR, Peachy NS. Pharmacological analysis of the rat cone electroretinogram. *Vis Neurosci*. 2003;20:297–306.
52. Chow RL, Snow B, Novak J, et al. Vsx1, a rapidly evolving paired-like homeobox gene expressed in cone bipolar cells. *Mech Dev*. 2001;109:315–322.
53. Kitazawa K, Hikichi T, Nakamura T, et al. OVOL2 maintains the transcriptional program of human corneal epithelium by suppressing epithelial-to-mesenchymal transition. *Cell Rep*. 2016;15:1359–1368.
54. Roca H, Hernandez J, Weidner S, et al. Transcription factors OVOL1 and OVOL2 induce the mesenchymal to epithelial transition in human cancer. *PLoS One*. 2013;8:e76773.
55. Liu Y, Peng X, Tan J, Darling DS, Kaplan HJ, Dean DC. Zeb1 Mutant mice as a model of posterior corneal dystrophy. *Invest Ophthalmol Vis Sci*. 2008;49:1843.
56. Liskova P, Dudakova L, Evans CJ, et al. Ectopic GRHL2 expression due to non-coding mutations promotes cell state transition and causes posterior polymorphous corneal dystrophy 4. *Am J Hum Genet*. 2018;102:447–459.
57. Nakamura M, Ofuji K, Chikama T, Nishida T. The NK1 receptor and its participation in the synergistic enhancement of corneal epithelial migration by substance P and insulin-like growth factor-1. *Br J Pharmacol*. 1997;120:547–552.
58. Muller L, Pels L, Vrensen G. Ultrastructural organization of human corneal nerves. *Invest Ophthalmol Vis Sci*. 1996;37:476–488.
59. Whiffin N, Minikel E, Walsh R, et al. Using high-resolution variant frequencies to empower clinical genome interpretation. *Genet Med*. 2017;19:1151–1158.
60. Liskova P, Gwilliam R, Filipec M, et al. High prevalence of posterior polymorphous corneal dystrophy in the Czech Republic; linkage disequilibrium mapping and dating an ancestral mutation. Janecke. *PLoS One*. 2012;7:e45495.
61. Héon E, Greenberg A, Kopp KK, et al. VSX1: a gene for posterior polymorphous dystrophy and keratoconus. *Hum Mol Genet*. 2002;11:1029–1036.
62. Eran P, Almogit A, David Z, et al. The D144E substitution in the VSX1 gene: a non-pathogenic variant or a disease causing mutation? *Ophthalmic Genet*. 2008;29:53–59.
63. Paliwal P, Singh A, Tandon R, Titiyal JS, Sharma A. A novel VSX1 mutation identified in an individual with keratoconus in India. *Mol Vis*. 2009;15:2475–2479.

Investigative Ophthalmology & Visual Science